Preliminary results for energy harvesting maximization with focus on heater control of batteries in nanosatellites

Edemar M. Filho, Sara V. Martinez, Leonardo K. Slongo, Eduardo A. Bezerra, Talita S. Possamai, Vicente P. Nicolau

UFSC

III IAA Latin American CubeSat Workshop - 2018

1 – Introduction
2 – Literature review
3 – Methodology
    3.1 – Thermal model
    3.2 – Electrical model
4 – Results
5 – Conclusions

Acknowledgements
References

INTRODUCTION

Orbit + Attitude → Irradiance

Governs the **temperature** and available **energy**.

Irradiance → Temperature & energy

May require thermal control to avoid **failure**, especially at **battery**.

Power Budget

Voltage of **battery,** voltage of **solar panels, EPS architecture,** DET, PPT models ...

Attitude model + Thermal model + Electrical model → Efficiency model

Heater operation coupled to **power system** to find **maximum efficiency** of EPS.

LITERATURE REVIEW

- **Warmer** photovoltaic panel and battery **reduces** the **performance**;
- **Battery** has **minimum** operational **temperature**, usually around **0℃** (charge) and **-20 ℃** (discharge);
- **DET** (Direct Energy Transfer) is a **simple** architecture for EPS where the **battery** is **parallel** to the **solar panels**
- **Trigger** of **tasks** to keep solar **panels** close to their **maximum power** point;

METHODOLOGY

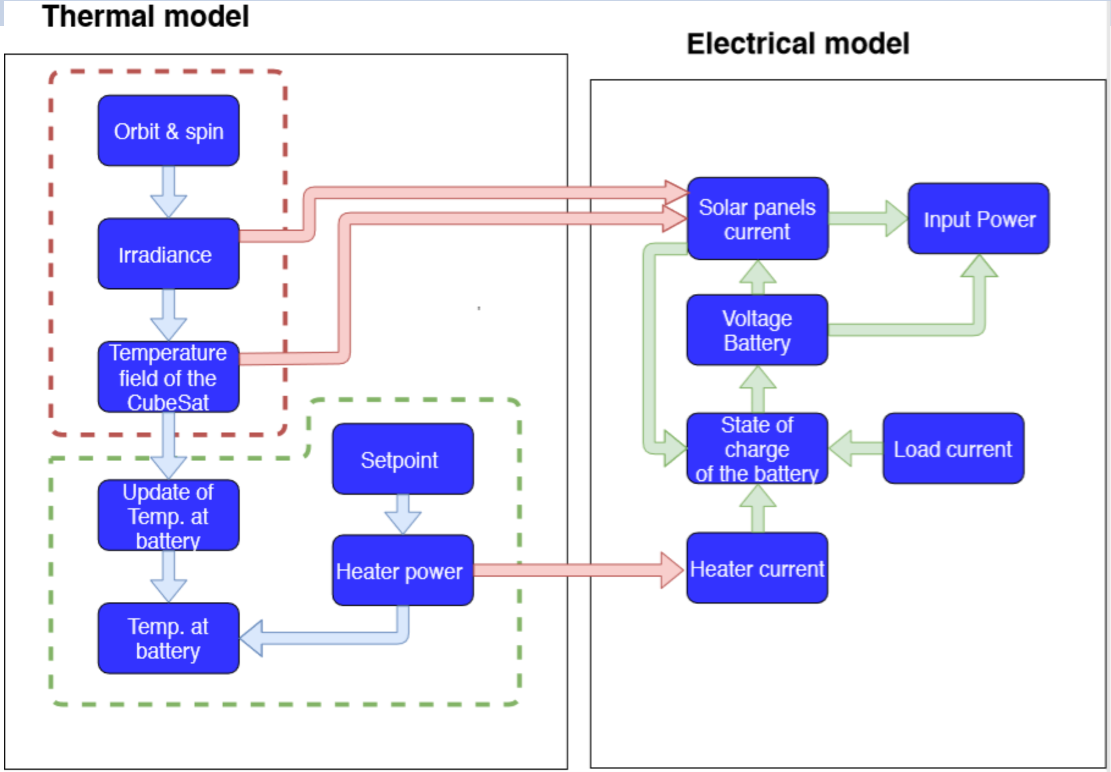

Figure 1 - Overview of the thermal and electrical model.

Thermal model: Numerical and analytical;
Inputs: Orbital parameters, attitude, geometry, design, and heater setpoint.
Outputs: irradiance, temperature of solar panels and power of heater.

Electrical model: Analytical.
Inputs: irradiance (solar flux), temperature (solar panels), power of heater.
Outputs: Battery voltage, power on solar panels.

METHODOLOGY: Thermal model

Orbit & attitude (UDF of ANSYS CFX):

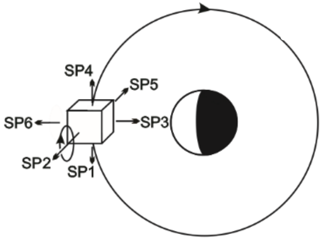

Altitude of 650 km, noon-midnight circular orbit, attitude of nadir.

Irradiance (UDF of ANSYS CFX): Solar flux, albedo and radiation from Earth.

Transient temperature field (ANSYS CFX, FVM):

$$\dot{E}_{in} - \dot{E}_{out} + \dot{E}_g = \dot{E}_{acu}$$

Temperature at battery (MATLAB):

$$T_{bat}(t) = \left[P_H(t) + \dot{E}_k(t) + \sum_{i=1}^{5} q_{r_i}(t)\right]\frac{\Delta t}{mc} + T_{bat}(t-1)$$

Heater power — Heat conduction — Radiation (Gebhart method)

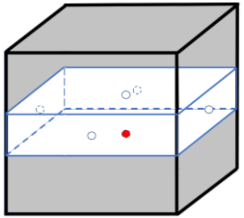

Algorithm:

if $T_{bat} < T_{set} + \Delta T$

$P_H = 1;$
$\Delta T = 5;$

else

$P_H = 0;$
$\Delta T = 0;$

end

Heater (P_H): 0-1 W

ΔT: 5 °C

Setpoint (T_{set}):

0°C, 5°C, 10°C

METHODOLOGY: Electrical model

State of charge (SoC): $\mathrm{SoC}(t) = \mathrm{SoC}(t_0) - \frac{1}{C_n}\int_{t_0}^{t} I_{bat}\, dt$

Battery charge current (I_{bat}): $I_{bat} = -[I_{SP} - (I_{heater} + I_{load})]$

Battery discharge current (I_{bat}): $I_{bat} = I_{heater} + I_{load} - I_{SP}$

Heater current (I_{heater}): $I_{heater} = \sqrt{\frac{P_H}{R}}$

Solar panel current (I_{heater}): $I_{SP} = I_{ph} - I_D\left[e^{\left(\frac{V_{bat}+I_{SP}R_s}{nV_t}\right)} - 1\right] - \frac{V_{bat} + I_{SP}R_s}{R_p}$

(T,I) (T) (T)

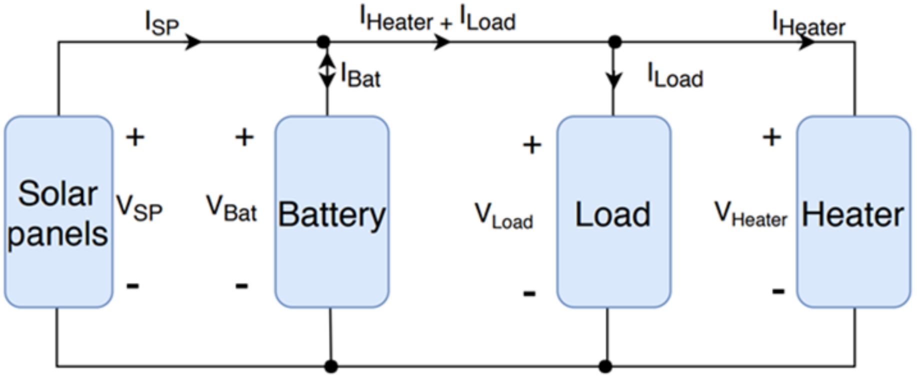

Figure 2: EPS simplified circuit diagram.

Quasi-cyclic behavior:
Previous temperature impacts in the following ones.

Heater also acts out of the eclipse:
Shadow is between 1840-3990 s and 7700-9850 s.

Higher setpoint require more time with heater on:
Upright ramp in the temperature relates to the heater on.

1W heater keeps the battery at safe temperature:
Usually the lower acceptable temperature is 0°C.

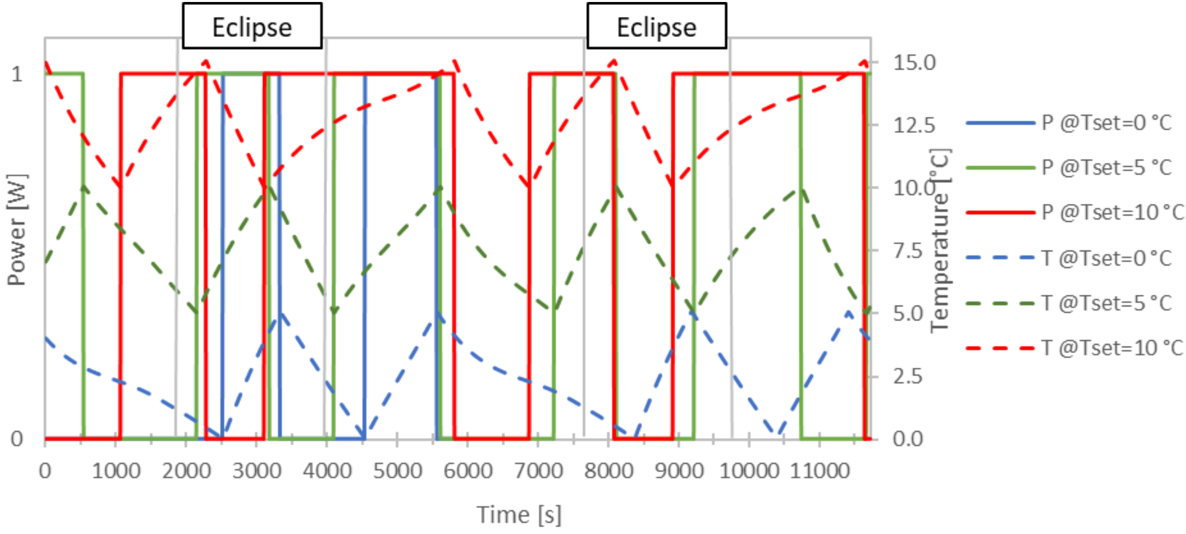

Figure 3 - Behavior of heater and temperature at battery at 8^{th} - 9^{th} run.

RESULTS

Heater and battery energy:
The power to operate the heater is greater than solar panels, which drives energy of battery.

Voltage drop:
The charge loss decreases the battery voltage up to 200 mV.

Support of solar panels:
The voltage drop is attenuated out of eclipse by the power of solar panels.

Higher the setpoint, higher the charge loss:
Only the minimum setpoint returns the state of charge to the initial point.

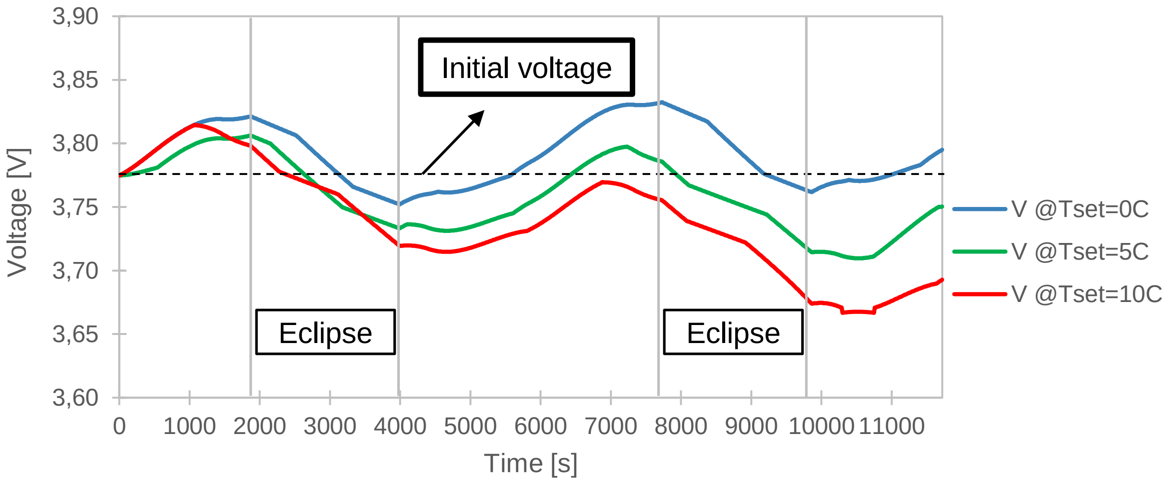

Figure 4 – Power of heater and voltage at battery at 8^{th} - 9^{th} run.

RESULTS

Non symmetric power input:
Before the shadow (hot satellite) the power input is smaller than after (satellite cold).

Small variation of energy due to battery voltage:

$T_{set} = 0°C$: 8.224 kJ and 8.149 kJ =100 %;
$T_{set} = 5°C$: 8.262 kJ and 8.230 kJ ≈100.7%;
$T_{set} = 10°C$: 8.262 kJ and 8.290 kJ ≈101.1%.

More power input with higher setpoint:
The voltage battery in these regions is closer to the point of maximum power of the panels.

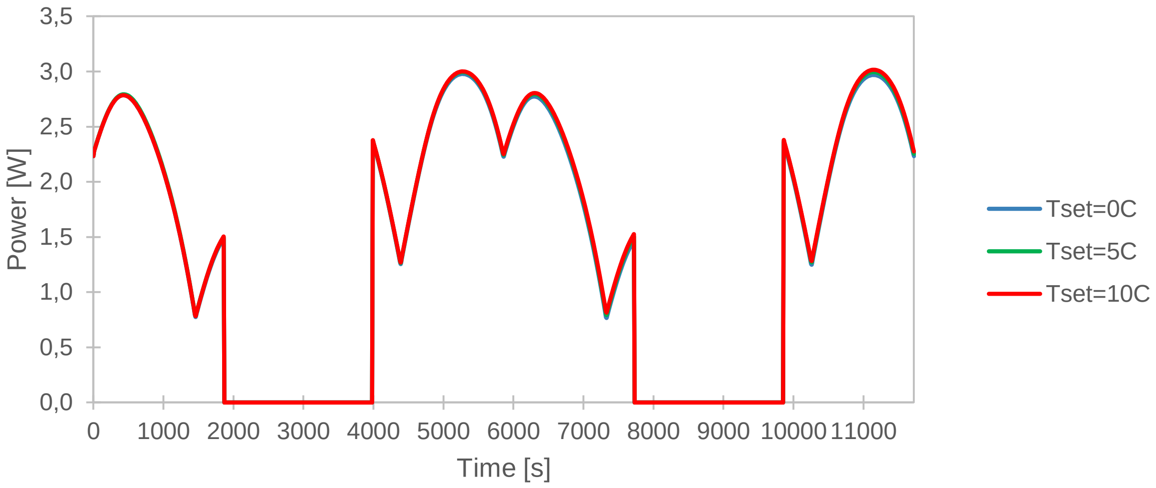

Figure 5 – Power input from solar panels at 8^{th} - 9^{th} run.

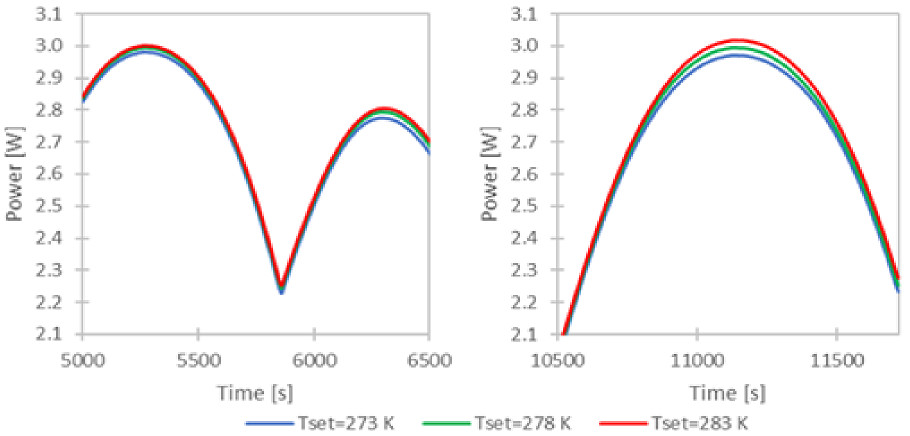

CONCLUSIONS

Energy harvesting model

Accurate energy models must consider the orbit, attitude, irradiance, temperature of solar panels and thermal control.

Scenarios

Within the tested setpoints, only the setpoint at 0°C was not critical for the battery voltage after two orbits.

Power of heater

Variations in the power consume of the heater impacts in the battery voltage and in the energy input

Control of setpoint

The heater control may optimize the battery voltage to operate the solar panels near their maximum power point.

ACKNOWLEDGMENTS

The present work was realized with the support of CNPq, National Council of Scientific and Technological Development – Brazil, for providing the scholarships under grant number 141276/2018-5, 141696/2017-6 and 150012/2018-7.

REFERENCES

[1]   Robert Burt, Distributed electrical power systems in cubesat applications, in Utah State University. theses ,Logan, Utah, 2011.
[2] K. B. Chin, E. J. Bronson, R. V. Bugga, M. C. Smart, S. C. Jones, F. C. Krause, Energy Storage Technologies for Small Satellite Applications, in: Proceedings of the IEEE, Feb. 2018. DOI: 10.1109/JPROC.2018.2793158
[3] G. Galatis, J. Guo, J. Buursink, Development of a solar array drive mechanism for micro-satellite platforms. Acta Astronautica, v. 139, n. Supplement C, p. 407-418, 2017. ISSN 0094-5765.
[4] D. Y. Lee, J. W. Cutler, J. Mancewicz, A. J. Ridley, Maximizing photovoltaic power generation of a space-dart configured satellite, Acta Astronautica, Volume 111, 2015, Pages 283-299, ISSN 0094-5765, https://doi.org/10.1016/j.actaastro.2015.01.022.
[5] N. Navarathinam, R. Lee, H. Chesser, Characterization of Lithium-Polymer batteries for CubeSat applications, Acta Astronautica, Volume 68, Issues 11–12, 2011, Pages 1752-1760, ISSN 0094-5765, https://doi.org/10.1016/j.actaastro.2011.02.004.
[6] A. Ali, M. R. Mughal, H. Ali, L. Reyneri, Innovative power management, attitude determination and control tile for CubeSat standard NanoSatellites, Acta Astronautica, Volume 96, 2014, Pages 116-127, ISSN 0094-5765, https://doi.org/10.1016/j.actaastro.2013.11.013.
[7] M. Uno, K. Ogawa, Y. Takeda, Y. Sone, K. Tanaka, M. Mita, H. Saito, Development and on-orbit operation of lithium-ion pouch battery for small scientific satellite "REIMEI", Journal of Power Sources, Volume 196, Issue 20, 2011, Pages 8755-8763, ISSN 0378-7753, https://doi.org/10.1016/j.jpowsour.2011.06.051.
[8] L.K. Slongo, S.V. Martínez, B.V.B. Eiterer, T.G. Pereira, E.A. Bezerra, K.V. Paiva, Energy-driven scheduling algorithm for nanosatellite energy harvesting maximization, Acta Astronautica, Volume 147, 2018, Pages 141-151, ISSN 0094-5765, https://doi.org/10.1016/j.actaastro.2018.03.052.
[9] D. G. Gilmore, Spacecraft Thermal Control Handbook: Fundamental technologies, 2nd ed., The Aerospace Corporation, California, 2002.
[10] W. J. Larson, J. R. Wertz, Space Mission Analysis and Design. Torrance, Calif: Microcosm, 1992. Print.
[11] R. Siegel, J. R. Howell, Thermal Radiation Heat Transfer, Hemisphere Publishing Corporation, Washington D.C., 1992.
[12] GOMSPACE. Datasheet - Battery. Available in: <https://gomspace.com/UserFiles/Subsystems/datasheet/gs-ds-nanopower-battery-17.pdf>, 2018.
[13] L. K. Slongo. Nanosatellite electrical power systems hardware architectures: an analysis on energy harvesting maximization through scheduling algorithm. Dissertation. Federal University of Santa Catarina. Brazil. 2017.
[14] Y-C Hsieh, T-Da Lin, R-Ji Chen, H-Yu Lin, Electric circuit modelling for lithium-ion batteries by intermittent discharging, Department of Electrical Engineering, National Dong Hwa University, Hualien, Taiwan.
[15] P. Sabine, P. Marion, A. Jossen, Methods for state-of-charge determination and their applications, J. Power Sources, 2001, 96, (1), pp. 113–120
[16] Y. Hu, S. Yurkovich, Battery state of charge estimation in automotive applications using LPV techniques, in: Proc. Amer. Control Conf., Baltimore, MD, USA, 2010, pp. 5043–5049.

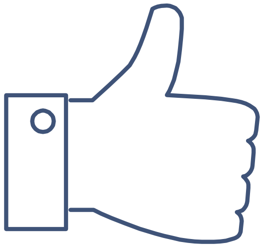

THANKS!

Any questions?

You can find me at:

ede.morsch@hotmail.com

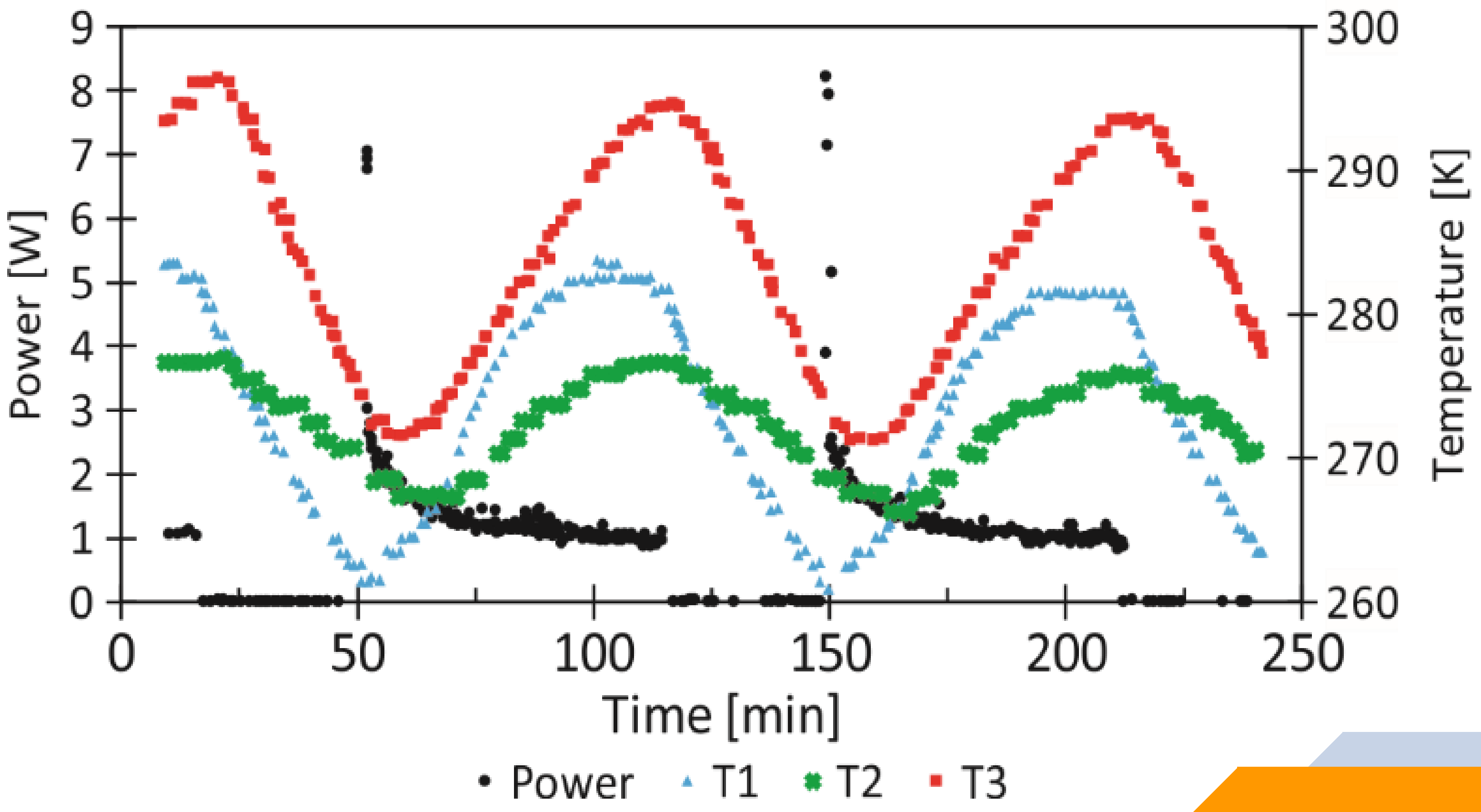
Power [W]
Temperature [K]
Time [min]
0
1
2
3
4
5
6
7
8
9
260
270
280
290
300
0
50
100
150
200
250
Power
T1
T2
T3

Current-Voltage & Power-Voltage Curve(230-20)